Formation processes at the early Late Pleistocene archaic human site of Lingjing, China

Hao Li[a,b], Zhanyang Li[c,d], Matt G. Lotter[e], Kathleen Kuman[f]

[a] Key Laboratory of Vertebrate Evolution and Human Origins, Institute of Vertebrate Paleontology and Paleoanthropology, Chinese Academy of Sciences, Beijing, 100044, China
[b] CAS Center for Excellence in Life and Paleoenvironment, Beijing, 100044, China
[c] Institute of Cultural Heritage, Shandong University, Jinan, 250100, China
[d] Henan Provincial Institute of Cultural Relics and Archaeology, Zhengzhou, 450000, China
[e] Department of Anthropology and Archaeology, University of Pretoria, Lynnwood Road, Pretoria, 0083, South Africa
[f] School of Geography, Archaeology and Environmental Studies, University of the Witwatersrand, Johannesburg WITS, 2050, South Africa

Abstract

Lingjing, located in northern China, is an open-air spring site dated to ~ 0-125 ka through Optically Stimulated Luminescence (OSL) dating. Two late archaic human crania, which possess a mosaic of features indicative of both eastern Eurasian and Neanderthal ancestry, were excavated from the site, along with abundant animal fossils and stone artifacts. Despite Lingjing's obvious significance, detailed analyses of the processes that have influenced site formation and modification have not yet been performed. In this paper we provide an interpretation of the depositional context at Lingjing and we also provide an assessment of the level of site disturbance, both during and post-deposition. Sedimentary and archaeological indicators are employed in this study, and results show that there is differential modification of the stratigraphic horizons, primarily between lower layer 3 and the overlying upper layers 2 and 1. Although this disturbance is apparent, overall its extent is limited. The findings in this study therefore confirm that assemblage integrity at Lingjing is high, and that behavioural information is well preserved.

Highlights

- Sedimentary and archaeological indicators show that there is differential modification of the stratigraphic horizons at the site of Lingjing.
- The Lingjing site was influenced by the depositional context of a spring pool, but the integrity or *in situ* nature of the assemblage was not significantly altered.
- A variety of activities was carried out at Lingjing over a relatively long period of time.
- Our analysis at Lingjing provides a valuable reference and methodological framework for site formation studies in China.

Keywords

Late Pleistocene, Lingjing, China, late archaic *Homo*, spring, site formation processes

1. Introduction

Biotic and abiotic agents frequently play a role in the preservation and subsequent modification of Paleolithic sites, patterning deposits in a way that reflects their influence. The study of site formation processes is therefore essential if we are to reliably decipher these patterns, and distinguish between those created by cultural activities, non-cultural (natural) forces, and distinguishing the relative contribution of each, when applicable (Schick, 1991). Early site formation studies in East Africa, which focused on Olduvai Gorge (Leakey, 1971; Hay, 1976; Potts, 1988; Petraglia and Potts, 1994), Olorgesailie (Isaac, 1967), Koobi Fora (Harris, 1978), Isimila (Howell et al., 1962), and Kalambo Falls (Schick, 1984; 2001), have been fundamental in promoting such analysis, and have thus stimulated similar research efforts in other geographic regions. As a result, site formation studies have progressed dramatically and now incorporate a far wider range of analytical techniques and applications.

Several geoarchaeological techniques are key when implementing a detailed analysis of Palaeolithic site formation and modification. For example, sediments are frequently analyzed for grain size, magnetic susceptibility, micromorphology, geochemical components, and mineral elements (e.g., Goldberg, 1979; Schiffer, 1983; Stein, 1987; Catt, 1999; French, 2003; Garrison, 2003; Morton, 2004; Ellwood et al., 2004; Goldberg and Macphail, 2006; Stahlschmidt et al., 2015; Toffolo et al., 2016; Campaña et al., 2016). Artefact properties, such as size profiles, abrasion, rounding, spatial distributions, and orientations, are commonly used as proxies of preservation for archaeological assemblages (e.g., Isaac, 1967; Schick, 1984, 1986; Bertran and Texier, 1995; Shea, 1999; Lenoble and Bertran, 2004; McPherron, 2005; Kuman and Field, 2009; Bernatchez, 2010; Braun et al., 2013; Hovers et al., 2014;

Lotter et al., 2016). With reference to the latter, in recent years spatial analysis using Geographic Information System (GIS) techniques has increasingly been used (Alperson-Afil et al., 2009; Benito-Calvo and de la Torre, 2011; Gallotti et al., 2011; Böhner et al., 2015; de la Torre and Wehr, in press).

However, compared with other regions, site formation studies in China have received less attention, and until recently only a few contributions have been made (see Pei et al., 2014, 2015; Li et al., 2016; Song et al., 2017). By utilizing multiple site formation indicators in this paper, we aim to provide a new case study here for such research, which we hope will further promote the practice of Palaeolithic site formation studies in hina

Our study site is Lingjing (34°04'08.6" N, 113°40'47.5" E), which is located in Henan Province in northern China (Fig. 1). It has been excavated regularly since 2005, and recently two early Late Pleistocene (105-125 ka) archaic hominid crania have been reported (Li et al., 2017). In addition to hominid fossils, abundant animal bones and stone artifacts were also excavated from the site (Li et al., 2007, 2010). Although Lingjing has played a significant role in understanding human physical and behavioral evolution, in this transitional Middle to Late Pleistocene period, detailed analysis of the formation and transformation of the site has not yet been undertaken. Preliminary stratigraphic analysis indicates that the site of Lingjing formed near to an area of pooling water, presumably fed from a nearby spring (Li et al., 2017). The site has thus, very likely, been influenced by hydraulic action. Therefore, our purpose here is to provide a detailed understanding of the depositional context so that we can better understand the cultural patterns preserved at the site. Specifically, we will answer two questions: has the site experienced post-depositional disturbance; if so, to what extent has the site been altered and its integrity affected?

Figure 1. A shows the general location of Henan Province within China, and B shows the general location of Lingjing within Henan Province. C shows the detailed topography around Lingjing. D shows the 2017 excavation area at Lingjing., indicated by the yellow rectangle.

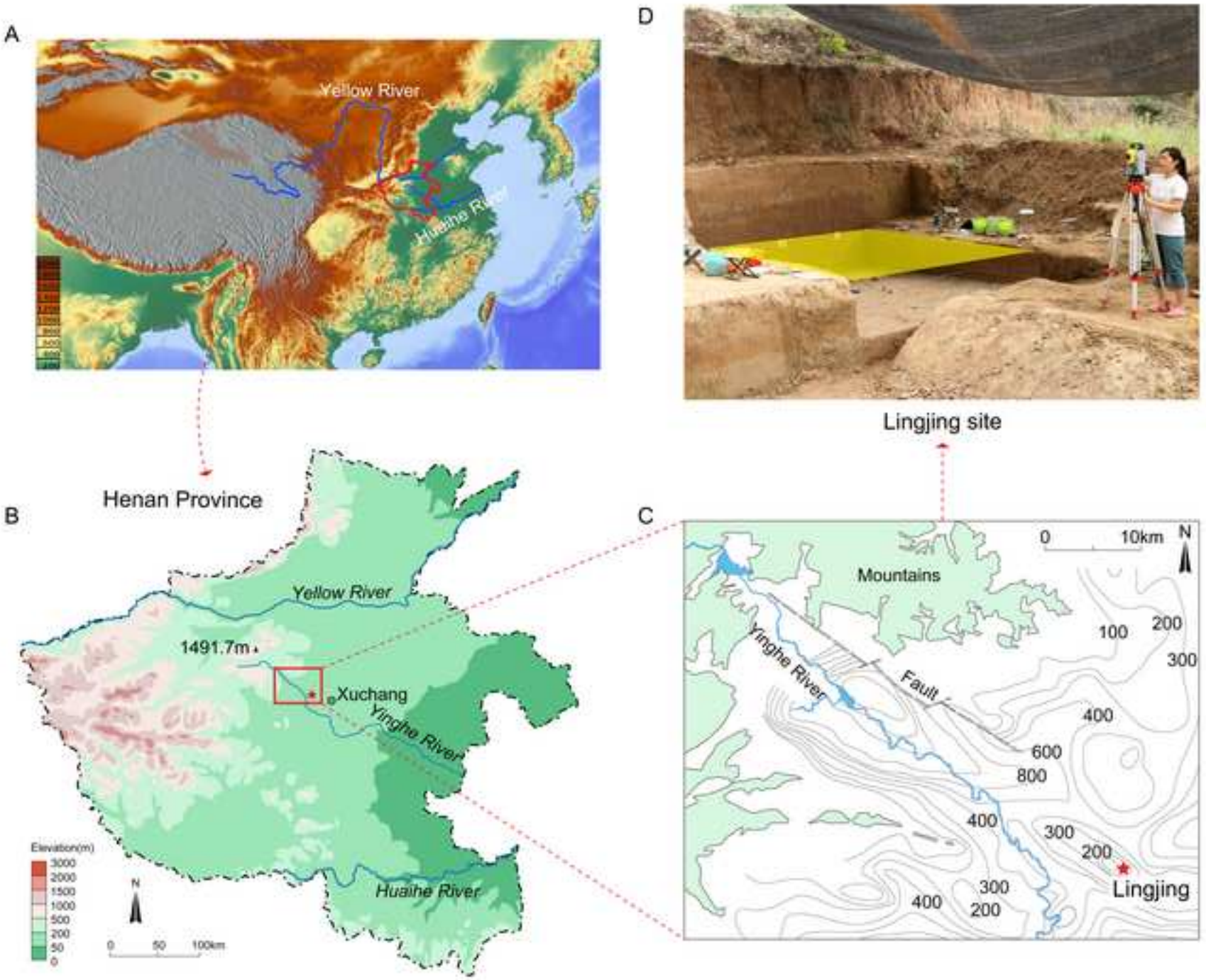

1.1. Geomorphology of the Lingjing region

The site of Lingjing is located to the west of the town of Lingjing, in Xuchang City of Henan Province. The site is also named Lingquan, which means Ling Spring in Chinese. The formation of the ancient spring here is closely related to the development of a fault that trends northwest-southeast (see Li, 2009 for a description; Fig. 1C). From a wider geomorphological perspective, the Lingjing region is situated in a transitional area between the Qinling Mountains to the west and China's Central Plain to the east, and it is dominated by undulating hillocks (Fig. 1A-C). The site of Lingjing is located within a lowland depression, which provides a favorable point on the landscape for gathering spring water (Fig. 1C); this spring opening is still present at the site today (Li et al., 2017). In addition, the site is also located at the most eastern boundary of the eolian loess deposits (Liu, 1997). The loess, which consists of silt, can either be directly deposited by wind or transported into the spring pool by flowing water, thus providing a source for the spring sediments.

Mammalian fossils discovered at Lingjing have helped us to reconstruct the paleoenvironment of the site. The *Viverra* cf. *zibetha* and *Ursus* sp. indicate the existence of a forest, while the *Palaeoloxodon* sp., *Coelodonta antiquitatis*, *Sus lydekkeri* and *Cervus elaphus* reflect a semi-open landscape; the large number of *Pachycrocuta* cf. *sinensis*, *Equus caballus*, *Equus hemionus* and *Bos primigenius* are indictors of a grassland environment (Li and Dong, 2007). Overall, these Lingjing fauna demonstrate a grassland-dominated ecological environment, with a mosaic of scattered forest and mixed forest vegetation (Li and Dong, 2007). This diversity of vegetation, coupled with the high-quality and readily available spring water, is very likely what attracted humans and animals to Lingjing.

1.2. Stratigraphy and chronology of Lingjing

Currently, Lingjing is well-known due to the discovery of two archaic human crania, which possess a mosaic of morphological features of both eastern Eurasian and Neanderthal ancestry. The Lingjing stratigraphy is divided into four layers. From the bottom to the top occurs: the lowest brownish red silt layer, sterile of all finds, with a thickness of ~ 5 cm; the overlying grayish green silt layer formed by spring

Figure 2. A shows the vertical distribution of finds throughout the sequence. Triangles show the stone artifacts while the round circles show fossilized bones. The light blue band shows the relatively sparse distribution of remains between 113.4-113.6 m. B shows the Lingjing stratigraphy and the division of four depositional layers. The vertical red and white bar (1.1 m in length) shows the sedimentary sample locations.

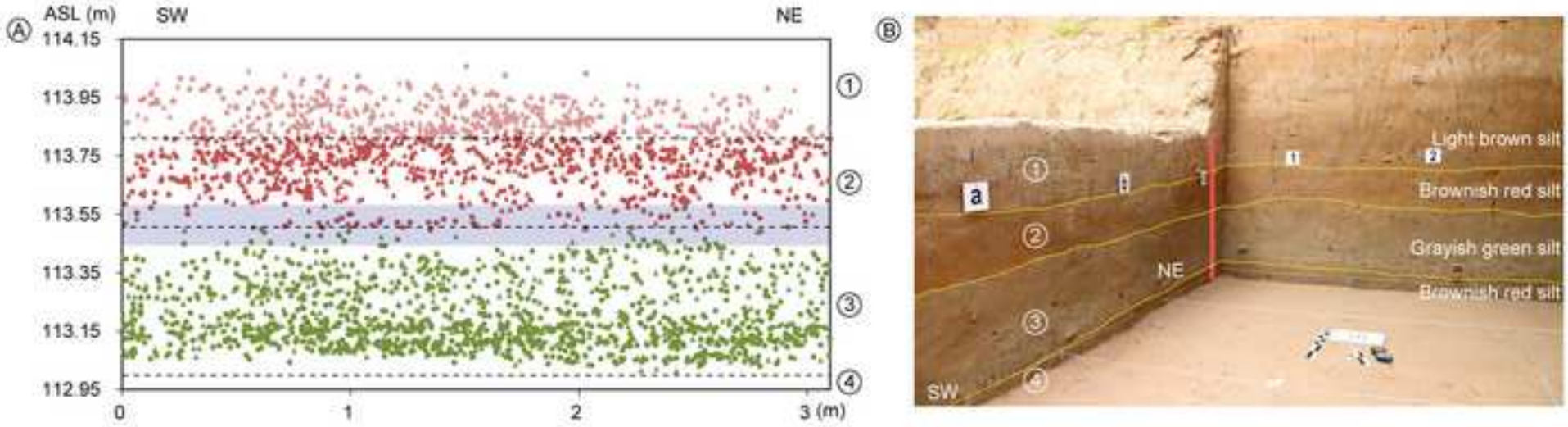

sedimentation (Li et al., 2017), with a thickness of ~ 50 cm; the brownish red silt layer, with a thickness of ~ 35 cm; the top layer, a relatively light brown silt, with a thickness of ~ 25 cm (Fig. 2). The latter three layers contain abundant fossils and artifacts. It is important to note that the schematic stratigraphy at Lingjing described by Li et al. (2017) was reconstructed from a wide regional perspective, including both historical and Neolithic cultural deposits near to the site. Based on the lithological and elevational comparisons, the grayish green silt layer 3 was assigned to layer 11 in Li et al. (2017), and from it the human crania were excavated and dated on five samples to ~ 105-125 ka (see Li et al., 2017 for a detailed description of the dating process). Layers 2 and 1 identified in this paper are equivalent to the lower layer 10, but only one sample collected from layer 10 has been dated to ~ 93±5 ka (Li et al., 2017). Therefore in this paper, we use a general age range of 90-125 ka for the deposits in layers 3 to 1, equivalent to the warm Marine Isotope Stage (MIS) 5 (Bradley, 2015). This period is linked to the dispersal of modern humans out of Africa (Bae et al., 2017), which consequently makes Lingjing a significant site when discussing the evolutionary background of modern humans in northern China.

2. Materials and methods

2.1. Materials

For this research we chose to re-excavate Lingjing from May to July, 2017, using the necessary equipment and recording new data that would be appropriate to facilitate the detailed site formation analysis. In total, just over 9 m2 were excavated to a depth of 1.1 m, dug in 5 cm horizontal spits (intervals).

In total, 3894 specimens were excavated from the site and among these 2148 are animal bones and 1746 are stone artefacts. Various types of artifacts are identified and vein quartz is the overwhelmingly dominant raw material (91.2%) (Table 1). Although all remains were spatially recorded during the excavation, some very small specimens < 5mm were retrieved during sieving, and thus the corresponding coordinate information was lost for 440 bones and 369 lithics; the final number of specimens plotted with a total station was 3085. A compass and an electronic inclinator were used to measure the long axis orientation and plunge of both lithics and bones. Only specimens with an obvious long axis and with lengths larger than 2 cm were chosen for recording, as suggested Lenoble and Bertran (2004). In total, 400 specimens were recorded (364 for bones and 36 for lithics) and 44 sedimentary samples were collected from the western stratigraphic profile, with an interval of 2.5 cm for each sample throughout the 1.1 m sequence (Fig. 3). These 44 samples have been used for the sedimentary analysis.

2.2. Methods

The detailed indicators used in this paper are presented below. The grain size, magnetic susceptibility and X-ray diffraction (XRD) analyses were performed at the Institute of Earth Environment, Chinese Academy of Sciences. The X-ray fluorescence (XRF) analysis was performed at the Institute of the Geological and Mineral Experiments of Shaanxi Province.

2.2.1. Grain size of sediments

Grain size is a commonly used indicator in sedimentological analysis, since changes in grain size respond directly to a change in the dynamics of hydraulic flow (Xiao et al., 2013). Coarse grain sizes correspond with stronger flow, while finer grain sizes, such as silt and clay, are associated with relatively weak flow that will have

Table 1. Lingjing artifact types grouped by raw material. Some flakes, flake fragments and split flakes are also less than 2 cm in size but were classed with the types due to their clear features. Misc. = miscellaneous.

	Quartz	Sandstone	Quartzite	Basalt	Total	%
Cores	43		2		45	2.6%
Flakes	92	3	31	3	129	7.4%
Flake fragments	34	2	18	5	59	3.4%
Split flakes	14	1	8	1	24	1.4%
Debris	1055		46		1101	63.1%
Chunks	257	11	21		289	16.6%
Formal tools	63		1		64	3.7%
Misc. retouched tools	34				34	1.9%
Unmodified pebble	1				1	0.1%
Total	1593	17	127	9	1746	
%	91.2%	1.0%	7.3%	0.5%		

Figure 3. The graph at left shows (from left to right) changes in mean grain size, the proportions of silt and sand, magnetic susceptibility, the ratio of Fe^{3+}/Fe^{2+}, and the Chemical Index of Alteration (CIA) of sedimentary samples through the sequence. Mean values of each item for layers 1, 2 and 3 are shown in the middle of each layer. At right, the location of the 44 sedimentary samples collected from the western profile in the 2017 excavation is shown.

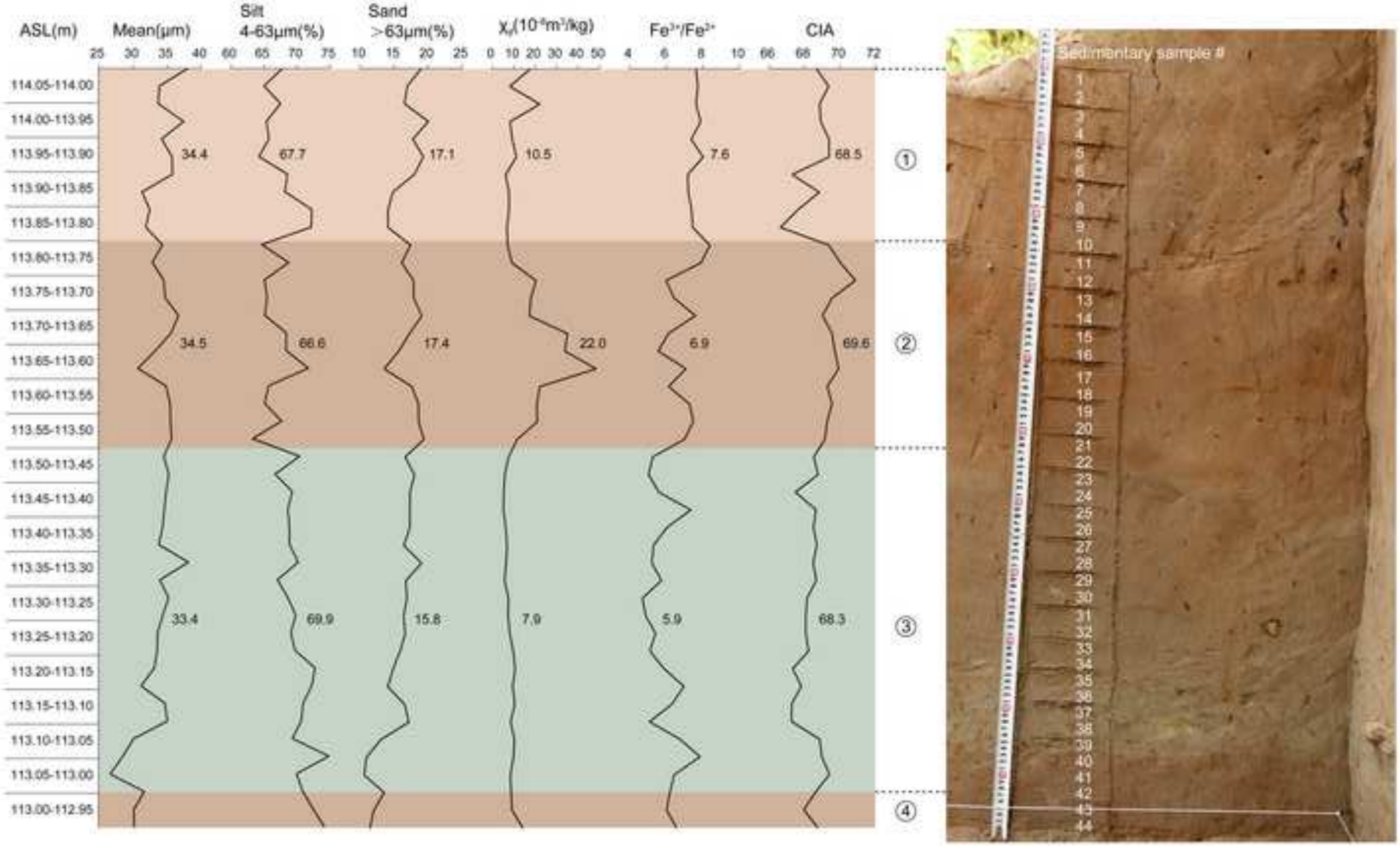

little or no influence in altering the site (Lerman, 1978). Mean grain sizes and size ranges for each sample are calculated, and line graphs are used to present the grain size changes throughout a sequence of deposits. A Malvern Mastersizer 2000 laser grain size analyzer, which has a measurement range of 0.02-2000 μm and a repeated measuring error of less than 2%, was used for our analysis. Before measuring, the samples were pretreated with H_2O_2 and HCl to remove organic matter and carbonate, and then with $(NaPO_3)_6$ solution to disperse ultrasonically (Lu and An, 1998; Liu et al.,

2.2.2. Magnetic susceptibility

Magnetic susceptibility is another commonly used technique that can indicate changes in depositional and climatic environments. Generally speaking, a high value of magnetic susceptibility is related to a humid and warm climate, whereas a lower value corresponds with a dry and cool climate (Heller and Liu, 1982, 1986; Liu et al., 1995; Maher and Thompson, 1995). Relevant studies of lacustrine deposits also show that high magnetic susceptibility has a correlation with warm and rainy seasons, which can provide greater energy for the deposition of sediments containing magnetic minerals (Dearing and Flower, 1982; Hu et al., 1998). However, the dissolution of magnetic minerals under relatively calm and stable lacustrine conditions can also reduce the magnetic susceptibility (Chen et al., 1995). Sedimentary samples used for laboratory analysis were ground to powders and then measured using a Bartington MS 2 meter under mass-specific low frequency (χ_{lf}, 470 Hz) magnetic susceptibility.

2.2.3. X-ray fluorescence (XRF) analysis of geochemical compositions

XRF is used to detect the proportion of different geochemical components in a sediment sample and the results are usually presented in the form of oxide percentages (Table 2). The combination of some oxides can provide robust information on environmental change (e.g., the Eluvial Coefficient and the Residual Coefficient, Zhao et al., 2004; Yang et al., 2016). Here we use the Chemical Index of Alteration (CIA) to indicate the degree of weathering in the sedimentary samples

Table 2. Geochemical element compositions of the sedimentary samples at Lingjing. Numbers are in %.

Sample #	SiO_2	Al_2O_3	Fe_2O_3	FeO	MgO	CaO	Na_2O	K_2O	MnO	TiO_2	P_2O_5	LOI
Layer 1												
1	72.24	11.13	3.31	0.39	1.18	0.99	1.66	2.42	0.037	0.61	0.13	5.75
2	73.16	11.51	3.26	0.38	1.22	1.00	1.58	2.50	0.050	0.63	0.13	4.42
3	72.92	11.42	3.39	0.40	1.21	1.09	1.56	2.52	0.062	0.64	0.17	4.46
4	73.43	11.21	3.33	0.38	1.17	0.99	1.56	2.50	0.057	0.63	0.13	4.46
5	72.80	11.40	2.95	0.36	1.16	0.97	1.58	2.49	0.079	0.63	0.12	5.33
6	73.07	11.56	3.30	0.37	1.21	1.04	1.54	2.52	0.063	0.64	0.15	4.40
7	72.60	11.39	3.11	0.39	1.20	1.44	1.60	2.49	0.069	0.64	0.41	4.50
8	73.09	11.50	3.28	0.41	1.22	1.14	1.55	2.51	0.063	0.65	0.21	4.21
9	72.59	11.31	3.20	0.39	1.19	1.29	1.63	2.49	0.10	0.63	0.30	4.73
10	72.45	11.32	3.15	0.38	1.19	1.59	1.57	2.50	0.082	0.63	0.50	4.48
Mean	*72.84*	*11.37*	*3.23*	*0.39*	*1.19*	*1.15*	*1.58*	*2.49*	*0.066*	*0.63*	*0.23*	*4.67*
Layer 2												
11	73.31	11.60	3.26	0.35	1.20	1.02	1.54	2.56	0.053	0.65	0.15	4.17
12	72.68	11.88	3.42	0.39	1.23	0.98	1.49	2.61	0.048	0.65	0.13	4.33
13	72.18	12.20	3.59	0.54	1.28	0.94	1.42	2.65	0.056	0.67	0.10	4.20
14	72.93	11.59	3.22	0.45	1.20	0.99	1.55	2.53	0.050	0.63	0.14	4.58
15	72.97	11.52	3.30	0.39	1.20	1.05	1.59	2.53	0.063	0.64	0.16	4.45
16	72.81	11.73	3.47	0.51	1.26	1.01	1.52	2.60	0.069	0.65	0.14	4.08
17	72.46	11.73	3.52	0.57	1.25	0.98	1.53	2.59	0.062	0.65	0.13	4.36
18	72.96	11.72	3.46	0.44	1.23	0.93	1.54	2.57	0.051	0.65	0.11	4.19
19	73.00	11.46	3.35	0.49	1.21	0.95	1.60	2.53	0.045	0.63	0.12	4.47
20	73.05	11.46	3.48	0.43	1.21	0.94	1.54	2.53	0.045	0.64	0.11	4.41
21	73.59	11.35	3.16	0.38	1.15	0.91	1.63	2.50	0.047	0.65	0.10	4.41
22	73.70	11.36	3.11	0.40	1.17	0.94	1.61	2.51	0.044	0.63	0.11	4.26
Mean	*72.97*	*11.63*	*3.36*	*0.45*	*1.22*	*0.97*	*1.55*	*2.56*	*0.053*	*0.65*	*0.13*	*4.33*
Layer 3												
23	73.91	11.16	2.87	0.49	1.15	0.97	1.65	2.50	0.040	0.62	0.14	4.34
24	73.85	11.40	2.97	0.53	1.20	1.00	1.60	2.58	0.042	0.64	0.16	3.87
25	73.16	11.32	2.99	0.48	1.20	1.28	1.62	2.56	0.055	0.63	0.33	4.24
26	73.46	11.37	3.02	0.37	1.19	1.01	1.63	2.56	0.040	0.63	0.17	4.41
27	73.46	11.30	2.95	0.44	1.17	0.97	1.66	2.56	0.038	0.62	0.14	4.54
28	73.68	11.32	2.95	0.50	1.18	0.96	1.63	2.57	0.038	0.63	0.13	4.25
29	73.65	11.19	2.95	0.51	1.16	0.95	1.65	2.54	0.041	0.62	0.13	4.44
30	73.48	11.27	3.00	0.47	1.17	0.96	1.64	2.54	0.053	0.63	0.13	4.52
31	72.70	11.02	2.77	0.53	1.13	0.94	1.72	2.49	0.041	0.60	0.13	5.79
32	73.05	11.00	2.76	0.51	1.12	0.96	1.69	2.51	0.049	0.61	0.13	5.45
33	73.38	11.21	3.01	0.50	1.16	1.03	1.67	2.55	0.047	0.64	0.17	4.47
34	73.84	11.08	3.01	0.53	1.14	0.97	1.65	2.54	0.052	0.62	0.14	4.27
35	73.40	11.06	3.00	0.46	1.14	1.17	1.68	2.51	0.050	0.62	0.26	4.50

36	73.33	11.21	3.18	0.41	1.17	1.10	1.64	2.58	0.043	0.62	0.23	4.36
37	73.41	11.05	3.09	0.44	1.14	1.12	1.70	2.55	0.051	0.63	0.22	4.45
38	74.71	10.75	2.66	0.47	1.07	0.98	1.78	2.47	0.038	0.62	0.15	4.15
39	72.87	11.54	3.46	0.46	1.26	0.95	1.56	2.71	0.050	0.65	0.12	4.22
40	72.07	11.55	3.66	0.42	1.28	0.94	1.54	2.71	0.042	0.64	0.13	4.87
41	72.44	11.87	3.51	0.49	1.32	0.95	1.50	2.78	0.052	0.66	0.12	4.17
42	73.12	11.43	3.31	0.48	1.24	0.94	1.59	2.69	0.057	0.64	0.12	4.23
Mean	*73.35*	*11.26*	*3.06*	*0.47*	*1.18*	*1.01*	*1.64*	*2.57*	*0.050*	*0.63*	*0.16*	*4.48*
Layer 4												
43	72.42	11.10	3.28	0.49	1.19	0.95	1.66	2.62	0.060	0.62	0.13	5.32
44	72.98	11.50	3.57	0.49	1.27	0.96	1.55	2.73	0.051	0.65	0.13	3.98
Mean	*72.70*	*11.30*	*3.43*	*0.49*	*1.23*	*0.95*	*1.60*	*2.67*	*0.056*	*0.64*	*0.13*	*4.65*
Mean for all data	*73.10*	*11.39*	*3.20*	*0.45*	*1.19*	*1.03*	*1.60*	*2.56*	*0.053*	*0.64*	*0.17*	*4.49*

(Nesbitt et al., 1982; Jahn et al., 2001); this index is calculated as: [Al_2O_3/Al_2O_3 +Na_2O+CaO+K_2O]×100. Al is accumulated in the later stage of weathering in a warm and humid environment, whereas Na, Ca and K can be easily leached out early in the weathering process. Thus, a higher CIA value indicates a warm and rainy climate, whereas a lower value corresponds with a dry, cool climate (Jahn et al., 2001). Other studies have shown that a CIA value lower than 65 indicates weak weathering under cool climatic conditions, while a value between 65 and 85 indicates modest weathering under a relatively warm climate (Feng et al., 2003; Li et al., 2013). The value ranges here provide a useful reference for understanding the environmental background.

A change in the proportion between Fe_2O_3 and FeO can also demonstrate a change in depositional environment. Fe_2O_3 is formed in an oxidizing environment with relatively turbulent water that can absorb more oxygen, while FeO is formed in a deoxidized environment with relatively calm water (Min and Chi, 2003). The potassium dichromate volumetric method is applied to determine the content of FeO (Yu et al., 1998). The proportion of Fe^{3+}/Fe^{2+} used in this paper demonstrates changes in the hydrodynamics at the site. Samples used for this study were ground to about 200 mesh size (< 75μm) and then measured using a PANalytical-Axios X-ray fluorescence spectrometer, with analytical uncertainties of less than 5%.

2.2.4. X-ray diffraction (XRD) analysis of mineral compositions

XRD is used to detect the minerals contained in sedimentary samples (Garrison, 2003, 2014; Goldberg and Macphail, 2006). The similarity or difference of mineral components in samples can reflect stability or change in the soil sources contributing to the sediments. In addition, some minerals such as the clay minerals of illite, montmorillonite and kaolinite, can also indicate the degree of weathering in archaeological sediments; their abundance can represent a higher degree of weathering. For XRD analysis, the samples were also ground to about 200 mesh size, and then these were measured using a Philips X'pert Pro (PW3071) X-ray diffractometer. Highscore software was used to semi-quantitatively calculate the

proportion of minerals in each sample.

In addition to this analysis conducted on the sedimentary samples, data were also collected on the archaeological materials, as discussed below.

2.2.5. Lithic assemblage size profiles

Experimental studies have shown that the size profile of a stone artifact assemblage is an effective indicator for site formation analysis (Schick, 1986; Kuman and Field, 2009; McNabb and Kuman, 2015). The small flaking debris (SFD) component of an assemblage is flaked material < 2 cm in length, and due to this small size it is most susceptible to relocation or transport away from the original site, frequently the result of a range of different processes, such as sheetwash or eolian dynamics (Schiffer, 1983; Kandel et al., 2003). When lithics are flaked on-site, there is a high proportion of SFD in a primary burial context, while proportions are lower in secondary or transformed contexts. In Schick's (1986) experimental work replicating East African lava artefacts, SFD ranged from 60-75% if loss of material is absent. However, considering the predominant use of vein quartz at Lingjing, here we use experimental data published by Kuman and Field (2009) for our comparisons. In their study, vein quartz cores that were knapped to exhaustion had a proportion of 87.1% SFD.

2.2.6. Orientation and plunge of lithics and bones

Orientation and plunge are widely used proxies that are extremely useful in site formation analysis. Orientation is measured for finds with a clear long axis, usually with a length that is 1.7 times the width. It is assumed that a random or uniform pattern of orientation indicates an undisturbed taphonomic environment, while a preferred pattern indicates the possible modification of the site (Bertran and Texier, 1995; McPherron, 2005). In fluvial contexts, the long axis orientation begins as perpendicular to the flow direction and becomes parallel to it with increasing velocities (Schick, 1986, 1987), while in a lacustrine context, the long axis orientation is parallel with the shoreline of the lake due to wave action (Morton, 2004). In

addition, mass movements, such as slides (of varying scales) or debris flows, can also cause a preferred orientation of artifacts along the slope (Bertran et al., 1997; Bertran and Texier, 1995, 1999). The degree of plunge can indicate the velocity of hydraulic flow. Steeper degrees correspond with stronger hydraulic flow, and vice versa (Schick, 1984, 1991). Rose diagrams are used to show the patterns of orientation and plunge. In addition, the Rao's test is applied for statistical confirmation of uniformity (Braun et al., 2013), along with the presence of mean vectors and circular standard deviations. If the *P* value is smaller than 0.05, there is a preferred pattern from a statistical perspective, which indicates that the site may have been modified.

2.2.7. Spatial distribution of lithics and bones

In general, a dense distribution of cultural remains in vertical space usually indicates a long-term or repeated occupation of a site, whilst a sparse distribution may imply infrequent use of a site. However, if the site is disturbed, the uneven vertical distribution of archaeological remains can also reflect the possible alteration of the site through time. In addition, patterns shown in horizontal space or plan view, such as a concentrated distribution in one particular area, can indicate both behavioral and transformational processes (e.g., fluvial re-concentrations or knapping locales, etc.). It is also noteworthy that various post-depositional processes can lead to the displacement of archaeological materials in the site. In general, these factors include animal trampling, fluvial forces, aeolian forces, bioturbation (termites, earthworms, plant roots, burrowing animals, etc.), downslope movements, and sediment re-consolidation and wetting and drying cycles (Cahen and Moeyersons, 1977; Moeyersons, 1978; Erlandson, 1984; McBrearty, 1990; Nielsen, 1991; Petraglia and Potts, 1994; McBrearty et al., 1998; Bertran and Texier, 1999; Kandel et al., 2003; Charlton, 2008; Forssman and Pargeter, 2014; Lotter et al., 2016). For analysis of spatial distribution patterns, in this study we have made density maps for each layer with the aid of GIS software. Kernel density maps are used for these plots, with a classification setting of 7 classes in equal intervals.

3. Results

3.1. Integrity of the site based on sedimentological indicators and implications for depositional background

Our analysis of 44 sedimentary samples at Lingjing shows that grain sizes are predominantly fine throughout the sequence, with an average of 33.8 μm falling within the lower size range for silt (16-63μm). These fine sediments indicate limited and low energy flow across the site. However, a detailed comparison of mean grain sizes in the different cultural layers demonstrates that, in contrast to layers 2 and 1, the grain sizes in layer 3 tend to be smaller. The mean grain size for layer 3 is 33.4 μm, while it is 34.5 μm and 34.4 μm for layers 2 and 1 respectively (Fig. 3). This is also reflected in the proportional changes for silt and sand, in the different layers. In particular, the mean proportion of fine grained silt in layer 3 (69.9%) is higher than it is in layers 2 (66.6%) and 1 (67.7%), whereas the coarse grained sand in layer 3 (15.8%) shows a lower mean proportion than in layers 2 (17.4%) and 1 (17.1%) (Fig. 3). Therefore, it is clear that layer 3 experienced relatively gentler hydraulic influences during formation of the deposit. In addition, Figure 3 shows that the bottom of layer 3 has the lowest mean grain size for all the layers (highest silt and lowest sand values), which illustrates a more stable depositional environment.

The curve for magnetic susceptibility throughout the sequence shows that the values are significantly increased in layer 2 (mean value=22.0 $10^{-8}m^3/kg$), in comparison with the lower values in layers 1 (mean value=10.5 $10^{-8}m^3/kg$) and 3 (mean value=7.9 $10^{-8}m^3/kg$) (Fig. 3). In contrast to all the other indices shown in Figure 3, magnetic susceptibility values exhibit the most remarkable variations between the layers, and can thus be regarded as an optimal index to represent changes in the depositional environment. The high values for magnetic susceptibility are closely related to a larger input of magnetic minerals due to stream flow (Dearing and Flower, 1982), which thus demonstrates relatively stronger turbulence in the spring pool. This finding correlates well with the grain size data for layer 2, which has the largest mean grain size, the highest mean percentage of sand and the smallest mean

percentage of silt, when compared with the other two layers. The lowest mean magnetic susceptibility values in layer 3, however, are probably influenced by a reduced input of water, which indicates a relatively calm and low energy depositional environment.

An unexpected phenomenon occurs in layer 2, at a depth of between 113.65-113.6 m, in which the magnetic susceptibility reaches the largest peak value, but this occurs in combination with the smallest value for the percentage of sand and the highest value for the percentage of silt, which is opposite to the overall trend observed in all the remaining layers. A possible explanation for this may be the result of denser vegetation during this rainy period in layer 2, which may have helped in the retention of coarser grained sand sitting on the surface.

A low value of Fe^{3+}/Fe^{2+} reflects a reducing environment, while a relatively large ratio can demonstrate a predominantly oxidizing environment. According to Figure 3, layer 3 has the lowest mean value (5.86) of Fe^{3+}/Fe^{2+}, in comparison to layers 1 (7.55) and 2 (6.91). Therefore, layer 3 was deposited in a relatively reducing, low-oxygen environment, which also seems apparent based on the clear grayish green color for the deposit. Such an environment is further related to calm and stable spring pool conditions, with less absorption of oxygen. In contrast, layers 1 and 2 likely correspond to a more turbulent spring pool environment in which more oxygen is taken up by the water, thus producing a high proportion of Fe^{3+}. It is also noteworthy that the values of Fe^{3+}/Fe^{2+} fluctuate within all layers of the three geological units (Fig. 3), thus demonstrating that internal variabilities still occur even within the overall trend of change for each layer.

The Chemical Index of Alteration (CIA) is usually used to demonstrate the extent of weathering in sedimentary samples. Results in Figure 3 show that layer 2 has a larger mean value (69.6) for the CIA than the other two layers (68.5 for layer 1 and 68.3 for layer 3; see Table 2 for raw data used to calculate the CIA value), which indicates that the formation of layer 2 took place in a wetter and more humid environment. In this environment, rainfall was probably greater and the shorelines of the spring pool probably altered more frequently. In addition, the higher CIA values in

layer 2 correlate positively to the values of magnetic susceptibility (Fig. 3). According to the criterion suggested by other scholars, a CIA value between 65-85 reflects a medium degree of chemical weathering and a warm temperate climate (Feng et al., 2003; Li et al., 2013). The CIA values in all three depositional layers of Lingjing fall well within the lower end of the range, and thus they demonstrate a generally warm temperate climate.

Analysis of the mineral components in all 44 samples shows that the composition is relatively stable in the different layers. Illite (mean 29.9%), quartz (mean 21.8%) and muscovite (mean 17.7%) are the main minerals for all layers. The other minerals, including albite, anorthite, biotite, augite, etc., often have proportions lower than 10% (Table 3). The similar mineral components and their proportions in different layers demonstrate a stable source of sediments from the nearby region, and there is a lack of extensive disturbance of the site caused by any intrusive sedimentary sources. On the other hand, the higher mean proportions of illite and quartz, in layers 2 and 1 when compared to layer 3, demonstrate that these two upper layers may have experienced more progressive weathering (Table 3). It is noteworthy that calcite is lacking in all three layers.

3.2. Integrity of the site based on archeological indicators

Analysis of the archaeological data provides a distinct perspective in understanding the formation processes of the site. Kuman and Field's (2009) experimental work reveals that a percentage of 87.1% for small flaking debris (SFD) is documented in primary knapping sites utilising vein quartz. The overall proportion of SFD at Lingjing is 69.5%, which is lower than the experimental result (Fig. 4). This may indicate that the humanly accumulated lithics have been altered by natural forces to some degree, or, that we are missing a portion of the knapping area. A comparison of the percentages of SFD in the different layers shows that layer 3 has a slightly larger proportion (71.1%) of SFD than layers 1 and 2 (69.1% and 67.9% respectively) (Fig. 4), which demonstrates that layer 3 possibly experienced slightly less modification, or that knapping was conducted within the immediate vicinity of

Table 3. Mineral components of the sedimentary samples at Lingjing. Numbers are in %.

Sample #	Quartz	Illite	Muscovite	Albite	Biotite	Orthoclase	Augite	Anorthite	Lepidolite	Mica	Berlinite	Monetite	Helvite
Layer 1													
1	15	40	19	9	—	4	—	13	—	—	—	—	—
2	19	21	10	4	7	2	—	—	—	11	—	25	—
3	28	28	24	7	11	3	—	—	—	—	—	—	—
4	21	25	22	6	4	3	—	—	—	7	13	—	—
5	27	36	23	7	5	3	—	—	—	—	—	—	—
6	31	33	17	9	3	3	5	—	—	—	—	—	—
7	14	28	20	6	9	2	3	7	—	11	—	—	—
8	20	26	20	6	9	2	3	5	—	8	—	—	—
9	27	33	24	6	4	3	3	—	—	—	—	—	—
10	21	35	21	7	3	2	3	7	—	—	—	—	—
Mean	*22.3*	*30.5*	*20.0*	*6.7*	*6.1*	*2.7*	*3.4*	*8.0*	—	—	—	—	—
Layer 2													
11	18	34	17	8	8	3	3	10	—	—	—	—	—
12	24	29	23	6	3	3	4	7	—	—	—	—	—
13	25	33	8	9	3	4	—	9	—	9	—	—	—
14	25	26	22	8	5	3	4	8	—	—	—	—	—
15	23	33	20	6	5	3	5	5	—	—	—	—	—
16	34	33	5	8	9	3	—	8	—	—	—	—	—
17	18	33	27	7	3	3	2	8	—	—	—	—	—
18	20	30	12	5	—	2	3	5	24	—	—	—	—
19	20	26	22	5	10	2	—	6	9	—	—	—	—
20	24	31	21	7	4	2	4	6	—	—	—	—	—

21	22	44	7	7	4	4	5	7	—	—	—	—	—
22	23	39	15	6	5	3	4	5	—	—	—	—	—
Mean	*23.0*	*32.6*	*16.6*	*6.8*	*5.4*	*2.9*	*3.8*	*7.0*	*16.5*	—	—	—	—
Layer 3													
23	22	34	20	6	2	4	—	6	7	—	—	—	—
24	20	28	18	6	—	4	3	7	12	—	—	—	—
25	22	31	13	7	6	4	3	6	8	—	—	—	—
26	15	26	20	8	4	3	2	9	13	—	—	—	—
27	20	24	18	5	4	2	4	5	8	—	—	—	13
28	22	29	19	7	4	2	1	8	8	—	—	—	—
29	20	25	19	7	7	3	—	8	11	—	—	—	—
30	23	30	21	7	—	2	—	6	11	—	—	—	—
31	22	29	26	7	—	3	—	6	8	—	—	—	—
32	22	27	20	7	3	3	3	7	9	—	—	—	—
33	22	27	17	6	6	3	3	6	10	—	—	—	—
34	20	26	17	6	4	1	—	6	7	—	—	—	12
35	24	29	18	7	5	2	2	6	9	—	—	—	—
36	24	29	22	6	3	2	—	5	8	—	—	—	—
37	19	32	12	7	8	2	4	7	7	—	—	—	—
38	23	26	19	4	4	2	—	4	18	—	—	—	—
39	22	30	18	6	7	2	3	5	7	—	—	—	—
40	20	26	13	7	4	2	—	6	8	—	—	—	14
41	17	26	11	7	7	2	4	8	7	—	—	—	12
42	19	27	11	5	5	2	3	6	9	—	—	—	14
Mean	*20.9*	*28.1*	*17.6*	*6.4*	*4.9*	*2.5*	*2.9*	*6.4*	*9.3*	—	—	—	—
Layer 4													

43	20	27	11	6	3	3	3	5	8	—	—	—	14
44	23	30	15	6	2	2	5	6	10	—	—	—	—
Mean	*21.5*	*28.5*	*13.0*	*6.0*	*2.5*	*2.5*	*4.0*	*5.5*	*9.0*	—	—	—	—
Mean for all data	*21.8*	*29.9*	*17.7*	*6.6*	*5.2*	*2.7*	*3.4*	*6.7*	*9.8*	—	—	—	—

Figure 4. Size profiles of stone artifacts in the different layers and in all layers combined are shown, with a comparison to the experimental results in vein quartz from Kuman and Field (2009).

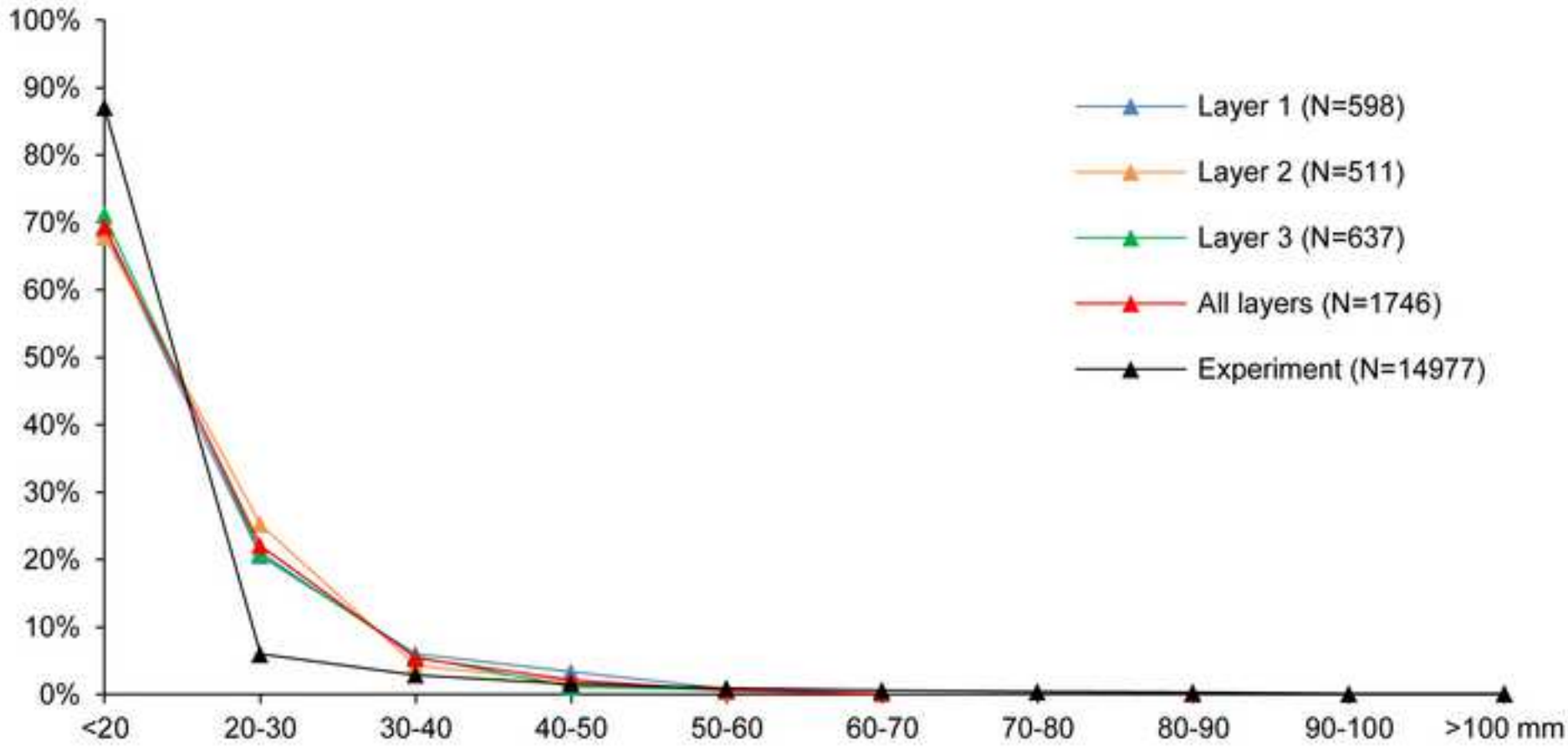

the excavated squares.

Specimens with lengths larger than 2 cm and a length/width ratio larger than 1.7 were used for orientation and plunge analysis, and in total this includes 364 bones and 36 stone artifacts. Rose diagrams of long axis orientations presented in Figure 6 show that the fabric of elongated specimens in layers 1 and 2 is relatively random, but certain concentrated orientations can still be observed: a main W-E direction for both layers and secondary directions of NW-SE for layer 1 and N-S for layer 2 (Fig. 5A,B). Regarding layer 3, bimodal patterns of NNE-SSW and NNW-SSE are relatively clear (Fig. 5C) Combined plots for artifacts, bones and all finds for the different layers also show the existence of a preferential pattern for long axis orientations (Fig. 5D-F). However, when comparing bones (Fig. 5E) and stones (Fig. 5D) separately we can see that the fabric pattern for stone artifacts is less clear than for bones, showing a preferential orientation different from the bones, and this is either caused by sample bias or some other currently undetected factors. Regarding plunge, in all cases there is a clearly clustered range between 0-10° (Fig. 5). However, in contrast with the mean plunge in layers 1 (14.8°) and 2 (14.6°), layer 3 has the lowest mean plunge of 10.6° (Table 4)., Considering the lack of oblique bedding throughout the layers, it is reasonable to infer that layer 3 formed during a relatively gentler e ositional en ironment

In order to quantitatively test our visual observations above, we conducted a Rao's uniformity test on the long axis orientation and plunge data. Results indicate that for both long axis orientation and plunge, all observed items have a *P* value smaller than 0.01, which means that the data are statistically significant (Table 4). Therefore, the archaeological remains at Lingjing were likely disturbed to a certain degree through the site formation processes.

The spatial distribution of remains in both vertical and horizontal space provides additional evidence for the site formation processes at play and the occupational history of the site (Fig. 2 and Fig. 6). The vertical distribution plot shows that there is a relatively sparse distribution of finds from the top of layer 3 to the lower part of layer 2, which corresponds to depths between 113.4-113.6 m (above sea level) (Fig.

Figure 5. Rose diagrams of long axis orientation and plunge for layers 1-3 are shown in A, B, C. D shows results for all stone artifacts combined, E for all fossils combined, and F for all finds in the layers combined.

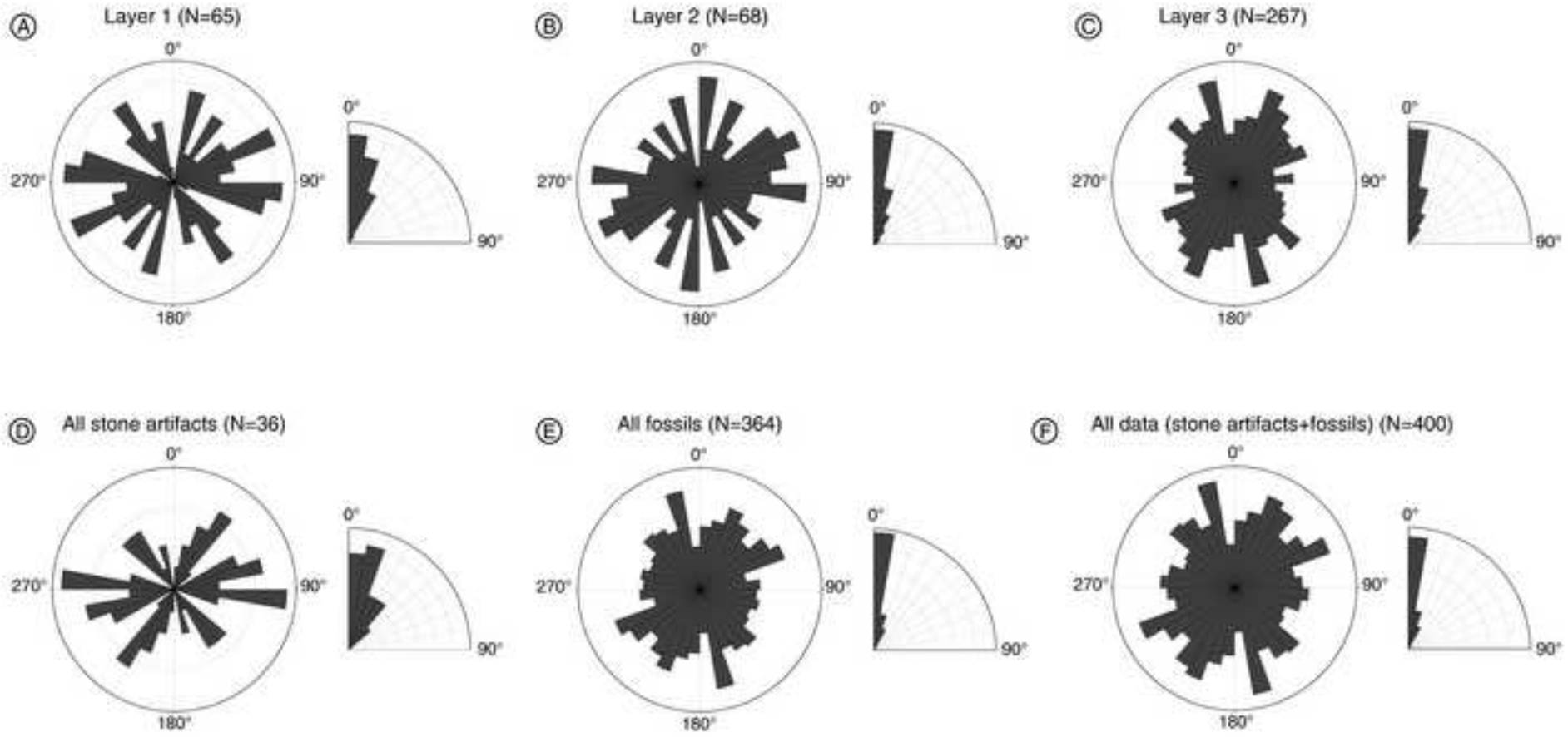

Table 4. Orientation and plunge of archaeological finds at Lingjing, along with the Rao's test for uniformity.

Assemblage	N	Orientation of long axis				Plunge			
		Mean vector	Circular SD	Rao's U	*p*	Mean vector	Circular SD	Rao's U	*p*
Layer 1	65	85.8	48.6	211.8	<0.01	14.8	10.5	308.8	<0.01
Layer 2	68	82.6	51.3	195.4	<0.01	14.6	16.8	293.4	<0.01
Layer 3	267	85.8	57.2	246.1	<0.01	10.6	15.7	309.1	<0.01
All stone artifacts	36	79.5	52.9	204.0	<0.01	20.4	13.5	302.2	<0.01
All fossils	364	86.5	56.2	243.3	<0.01	11.2	15.2	307.4	<0.01
All data	400	85.9	56.0	252.0	<0.01	12.0	15.3	305.8	<0.01

Figure 6. GIS-based density maps for all finds are shown for the different layers according to size intervals and all data combined. A-D show layer 1, E-H show layer 2, and I-L show layer 3.

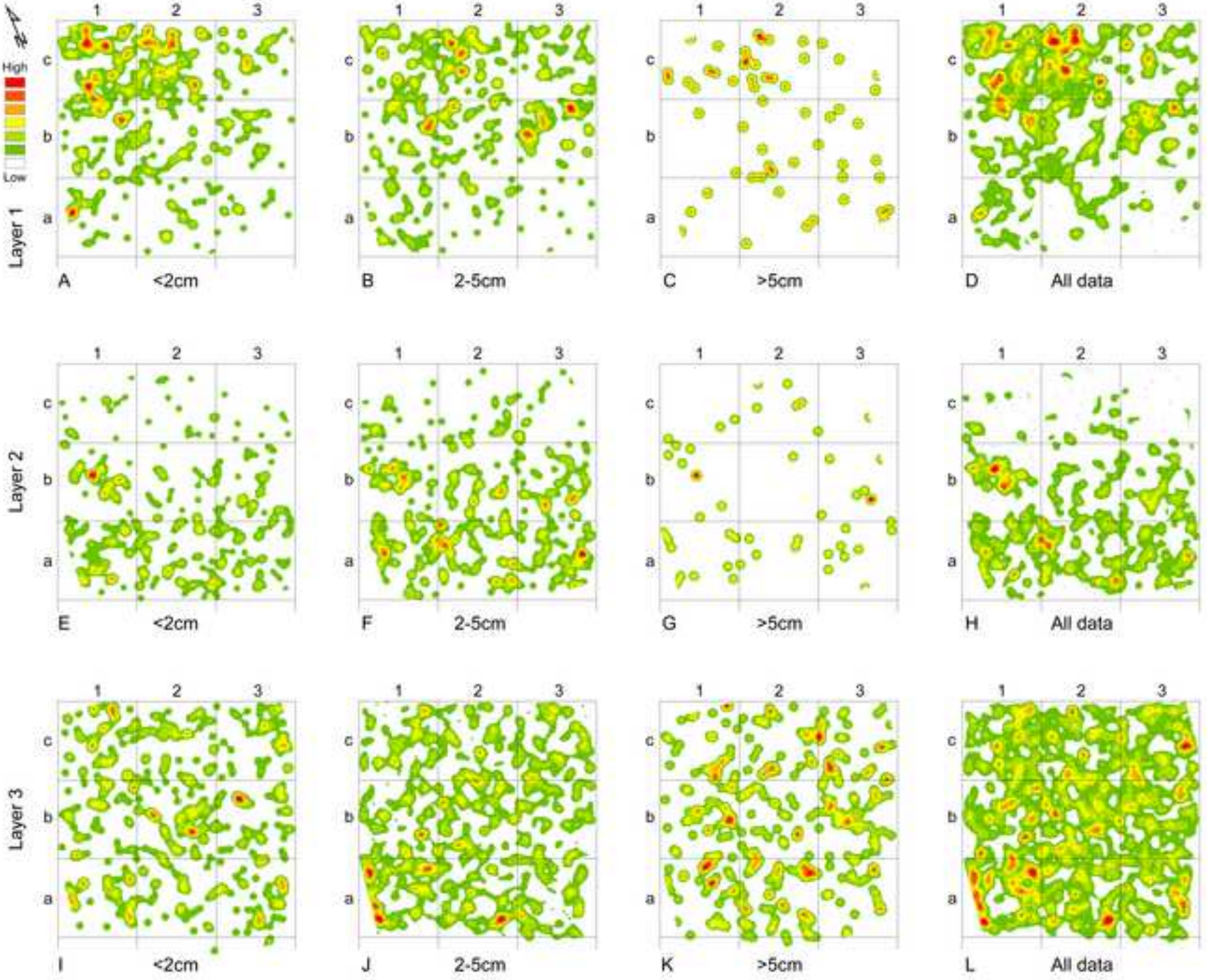

2A). Perhaps this relates to a relatively low frequency of human activity on site that occurred in the transitional stage of the depositional faces, but this assumption needs to be confirmed after our excavations have been expanded. However, it is clear that the remains are distributed continuously throughout the sequence, without any hiatus, which demonstrates that humans repeatedly visited the site for a relatively long period.

Based on our GIS analysis, density maps of the horizontal distribution of finds are provided by layer in Figure 6. Results show that layer 1 finds are concentrated in the northern portion of the excavated squares, while layer 2 exhibits a clustered area of finds in the southern squares (Fig. 6). Density maps of layers 1 (Fig. 6A-D) and 2 (Fig. 6E-H) plotted according to the size of the finds show a similar distribution pattern. The uneven distributions in layers 1 and 2 are possibly related to a certain degree of disturbance by natural agents, although the plotted area is small. The distribution of finds in layer 3 (Fig. 6I-L), however, is relatively uniform, which may indicate a less disturbed environment in the formation of this layer, or relate to a higher frequency of on-site activity across a larger area. We acknowledge, however, that our current interpretation of distributional patterns is based on only a limited excavation area, which may lead to bias. Expanded excavations in the future will be essential in providing more evidence.

4. Discussion

4.1. Hydrodynamics and the extent of its disturbance at Lingjing

The grayish green silt deposited in layer 3 provides strong evidence for the existence of a spring pool at Lingjing, thus supporting previous observations by Li et al. (2017). Layer 3 formed in a relatively closed and oxygen-poor environment, with a relatively high proportion of Fe^{2+}, creating the grayish green color of the deposits. The upper brownish red and light red silts of layers 2 and 1 were also deposited in a spring pool environment, but are characterized by a lack of calcareous leaching in the bottom

of these two layers. In the loess-paleosol sequence widely distributed in the Loess Plateau, it has been confirmed that paleosols were formed in relatively warm and humid periods, with layers of calcareous leaching typical of the bottom levels of the red colored paleosol sediments (Liu, 1985). Thus the bottom of layers 1 and 2 at Lingjing demonstrate the existence of water at the base of the red silt layers, which prevented the formation of calcareous sediment. The XRD analysis of mineral components also shows that there is a lack of calcite throughout the profile. Layer 3, which formed during a relatively stable depositional environment, is different from layers 2 and 1 as these were buried and subjected to fluctuating water due to the frequent rise and fall of the local water table. Regardless of these variations, an ancient spring pool existed at Lingjing for a long period, which must have been a major factor in attracting both humans and animals to the site. Meanwhile, the archaeological remains would inevitably have been influenced by the movement of water in the spring pool.

Based on various sedimentary indicators, layers 2 and 1 at Lingjing exhibit relatively stronger hydraulic flows, while layer 3 shows relatively weak hydrodynamics in terms of: the smallest mean grain size and proportion of silt; the lowest mean value of magnetic susceptibility; the lowest ratio of $Fe^{3+}/Fe^{2+;}$; and the lowest mean value for the Chemical Index of Alteration. On the other hand, grain sizes are dominated by fine silt in the different layers, indicating an overall weak hydraulic flow. The stable mineral components in the different layers further confirm a lack of intrusive agents that could have changed the depositional environment significantly.

Our analysis of archaeological remains also confirms a degree of disturbance by water during site formation, although the influence of hydraulic action in layer 3 is smaller than in layers 2 and 1, which is consistent with the sedimentary analysis. This evidence includes: the slightly higher proportion of small flaking debris (SFD) in layer 3 than in layers 1 and 2; a smaller mean plunge in layer 3 than in layers 1 and 2; an even distribution of remains in layer 3, versus a concentrated distribution of finds for layers 1 and 2. In general, however, disturbance in all three layers is limited,

especially considering the overall low values of plunge and the relatively high proportions of SFD. In summary, we can state that the Lingjing site was influenced by the depositional context of a spring pool, but the integrity or *in situ* nature of the assemblage was not significantly altered, and thus good behavioral information is preserved at the site.

4.2. Human behavior at the site of Lingjing

The fairly limited disturbance of Lingjing provides us with a relatively complete picture of human culture. Zooarchaeological analysis of the fauna from previous excavations indicates that *Equus caballus* and *Bos primigenius* are both dominant species. Based on a study of the mortality structure of these two species, adult individuals were preferentially hunted by humans (Zhang et al., 2009, 2011a; Li et al., 2011). Bones with cut marks account for approximately 13% of the entire faunal sample, with 98.5% of these marks located on the midshafts of long bones. Such a modification pattern on the bones and the paucity of carnivore tooth marks demonstrate that the Lingjing humans were the primary consumers of these animals (Zhang et al., 2011b). The modification and use of bone materials as tools are also confirmed at Lingjing by a preliminary microwear analysis, which suggests that these artifacts were used for boring, piercing and scraping (Li and Shen, 2010). In addition, the large number of fragmentary bones in the faunal assemblage suggests humans were accessing the marrow (Zhang et al., 2011a). Diverse types of stone artifacts, as shown both in the previous (Li et al., 2007, 2010) and current excavated samples (Table 1), indicate both the manufacture and probable use of stone tools on-site. The uninterrupted vertical distribution of remains throughout the sequence, along with the large number of faunal taxa recovered in previous excavations (Li and Dong, 2007), demonstrates that the site was occupied repeatedly over a relatively long period. As a consequence we can reasonably infer that a variety of activities was carried out at Lingjing over a relatively long period of time. However, it is hard to determine whether the people that inhabited the site belonged to one population group or

multiple, but based on the consistencies in lithic production strategies throughout the sequence (Li, 2007, 2010), we can at least suggest that people possessing the same technological tradition lived in the region for a long period.

Based on our current findings, and thus our improved understanding of the evolution of Lingjing, here we provide a preliminarily reconstruction of the site's depositional history. The lowermost layer 3 was initially deposited at the edge of the the shoreline, alongside the spring pool, and humans occupied the site and conducted various activities on dry land. Due to the fluctuation of the water level, this layer was frequently buried by relatively low energy water flow (both surface derived and subaqueous, from the spring itself). Layers 2 and 1 were also situated at the spring pool shoreline, which allowed for the recolonization of the region, but these layers were affected by increased fluctuations in the water level, more frequently than during layer 3; this led to greater deposit modification, through hydrodynamic processes. Above layer 1 there is an absence of cultural remains and the sediments are typical of the eolian loess deposits (Li et al., 2017), which indicates the disappearance of the spring pool and very likely the reason for its abandonment.

5. Conclusions

As we have stated at the beginning of this paper, the significance of site formation studies is high as it provides us with a better understanding of the depositional context of Paleolithic sites, allowing us to better understand their preserved cultural residues. Our analysis at Lingjing contributes to this topic by providing a valuable reference and methodological framework for site formation studies in China. Some of the results achieved in this paper also aid our understanding of the functions represented at the site and the environmental adaptations of humans living in the area. Further excavation and site formation analysis at Lingjing should provide additional evidence to support our interpretations.

Acknowledgements

We thank Prof. Hu Xiaomeng from the Shanghai Normal University for his help on

stratigraphic interpretation. This research has been funded by the Strategic Priority Research Program of the Chinese Academy of Sciences (No. XDA19050102), the Chinese Academy of Sciences Pioneer Hundred Talents Program, the Chinese Academy of Sciences Strategic Priority Research Program Grant (No. XDPB05), the Shandong University 111 Project (111-2-09), and the National Natural Science Foundation of China (41672020). MGL would like to acknowledge funding support provided by the National Research Foundation (NRF) of South Africa and the Palaeontological Scientific Trust (PAST) with its Scatterings of Africa programs. KK also acknowledges the NRF support (grant number 88480) for her collaborative work in China.

References

Alperson-Afil, N., Sharon, G., Kislev, M., Melamed, Y., Zohar, I., Ashkenazi, S., Rabinovich, R., Biton, R., Werker, E., Hartman, G., Feibel, C., Goren-Inbar, N., 2009. Spatial Organization of Hominin Activities at Gesher Benot Ya'aqov, Israel. Science 326, 1677-1680.

Bae, C.J., Douka, K., Petraglia, M., 2017. On the origin of modern humans: Asian perspectives. Science 358 (6368), eaai9067.

Benito-Calvo, A., de la Torre, I., 2011. Analysis of orientation patterns in Olduvai Bed I assemblages using GIS techniques: Implications for site formation processes. J. Hum. Evol. 61, 50-60.

Bernatchez, J.A., 2010. Taphonomic implications of orientation of plotted finds from pinnacle point 13B (Mossel bay, western Cape Province, South Africa). J. Hum. Evol. 59, 274-288.

Bertran, P., Hetu, B., Texier, J., van Steijn, H., 1997. Fabric characteristics of subaerial slope deposits. Sedimentology 44, 1-16.

Bertran, P., Texier, J., 1995. Fabric analysis: application to Paleolithic sites. J. Archaeol. Sci. 22, 521-535.

Bertran, P., Texier, J., 1999. Facies and microfacies of slope deposits. Catena 35, 99-121.

Böhner, U., Serangeli, J., Richter, P., 2015. The Spear Horizon: First spatial analysis of the Schöningen site 13 II-4. J. Hum. Evol. 89, 202-213.

Bradley, R.S., 2015. Paleoclimatology (Third Edition): Reconstructing Climates of the Quaternary. Academic Press, New York.

Braun, D.R., Levin, N.E., Stynder, D., Herries, A., Archer, W., Forrest, F., Roberts, D., Bishop, L., Mattews, T., Lehmann, S., Pickering, R., Fitzsimmons, K., 2013. Quat. Sci. Rev. 82, 145-166.

Cahen, D., Moeyersons, J., 1977. Subsurface movements of stone artefacts and their implications for the prehistory of Central Africa. Nature 329, 812-815.

Campaña, I., González, A., Benito-Calvo, A., Rosell, J., Blasco, R., Bermúdez de Castro, J.M., Carbonell, E., Arsuaga, J.L., 2016. New interpretation of the Gran Dolina-TD6 bearing *Homo antecessor* deposits through sedimentological analysis. Scientific Reports 6, 34799.

Catt, J.A., 1999. Particle size distribution and mineralogy of the deposits. In: Roberts, M.B., Parfitt, S.A. (Eds.), Boxgrove. A Middle Pleistocene hominid site at Eartham Quarry, Boxgrove, West Sussex. Archaeological Report 17. English Heritage, London, pp. 111-118.

Charlton, R., 2008. Fundamentals of fluvial geomorphology. Routledge, London.

Chen, F.H., Wang, S.M., Li, J.J., Shi, Y.F., Li, S.J., Cao, J.X., Zhang, Y.T., Wang, Y.F., Kelts, K., 1995. The magnetic stratigraphic study of the Nuoergai Lake in the Tibet Plateau. Sci. China Ser. D Earth Sci. 25 (7), 772-777.

de la Torre, I., Wehr, K., in press. Site formation processes of the early Acheulean assemblage at EF-HR (Olduvai Gorge, Tanzania). J. Hum. Evol. http://dx.doi.org/10.1016/j.jhevol.2017.07.002.

Dearing, J.A., Flower, R.J., 1982. The magnetic susceptibility of sedimenting material trapped in Lough Neagh, Northern Ireland, and its erosional significance. Limnol. Oceanogr. 27, 969-975.

Ellwood, B.B., Harrold, F.B., Benoist, S.L., Thacker, P., Otte, M., Bonjean, D., Long, G.J., Shahin, A.M., Hermann, R.P., Grandjean, F., 2004. Magnetic susceptibility applied as an age-depth-climate relative dating technique using sediments from

Scladina Cave, a Late Pleistocene cave site in Belgium. J. Archaeol. Sci. 31, 283-293.

Erlandson, J.M., 1984. A case study in faunalturbation: delineating the effects of the burrowing pocket gopher on the distribution of archaeological materials. American Antiquity 49, 785-790.

Feng, L.J., Chu, X.L., Zhang, Q.R., 2003. Chemical Index of Alteration and its application in the debris rocks of Neoproterozoic. Frontier. Geol. 4, 539-544.

Forssman, T., Pargeter, J., 2014. Assessing surface movement at Stone Age open-air sites: first impressions from a pilot experiment in northeastern Botswana. Southern African Humanities 26, 157-176.

French, C., 2003. Geoarchaeology in action: studies in soil micromorphology and landscape evolution. Routeledge, London.

Gallotti, R., Mohib, A., Graoui, M.E., Sbihi-Alaoui, F.Z., Raynal, J.-P., 2011. GIS and intra-site spatial analyses: An integrated approach for recording and analyzing the fossil deposits at Casablanca prehistoric sites (Morocco). J. Geogr. Inform. Sys. 3, 373-381.

Garrison, E., 2003. Techniques in archaeological geology. Springer, Berlin.

Garrison, E., 2014. X-Ray Diffraction (XRD): Applications in Archaeology. In: Smith, C. (Eds.), Encyclopedia of Global Archaeology. Springer, New York, pp. 7929-7933.

Goldberg, P., 1979. Micromorphology of Pech-de-l'Azé II sediments. J. Archaeol. Sci. 6, 17-47.

Goldberg, P., Macphail, R.I., 2006. Practical and Theoretical Geoarchaeology. Blackwell Publishing, Carlton Malden, Oxford.

Harris, J.W.K., 1978. The Karari Industry. Its Place in East African Prehistory. Ph.D. Dissertation, University of California, Berkeley.

Hay, R.L., 1976. Geology of the Olduvai Gorge. University of California Press, Berkeley, Los Angeles, London.

Heller, F., Liu, T.S., 1982. Magnetostratigraphica dating of loess deposits in China. Nature 300, 431-433.

Heller, F., Liu, T.S., 1986. Palaeoclimatic and sedimentary history from magnetic susceptibility of loess in China. Geophy. Res. Lett. 13, 1169-1172.

Hovers, E., Ekshtain, R., Greenbaum, N., Malinsky-Buller, A., Nir, N., Yeshurun, R., 2014. Islands in a stream? Reconstructing site formation processes in the late Middle Paleolithic site of ‘Ein Qashish, northern Israel. Quat. Int. 331, 216-233.

Howell, F.C., Cole, G.H., Maxine, R., Kleindienst, Haldemann, E.G., 1962. Isimila, an Acheulian occupation site in the Iringa Highlands, Southern Highlands Province, Tanganyka. In: Mortelmans, G., Nenquin, J. (Eds.), Actes du IV-e Congres Panafricain de Prehistoire et de l'Etude du Quaternaire. Musee Royal de l'Afrique Centrale. Section III: Pre- et Protohistoire, Tervuren, pp. 43-80.

Hu, S.Y., Wang, S.M., Appel, E., Ji, L., 1998. The enrivonmental magnetic mechanism of the change of magnetic susceptibility in the lacustrine deposits at Hulun Lake. Sci. China Ser. D Earth Sci. 28 (4), 334-339.

Isaac, G.L., 1967. Towards the interpretation of occupation debris: some experiments and observations. Kroeber Anthropological Soc. Pap. 37, 31-57.

Jahn, B., Gallet, S., Han, J.M., 2001. Geochemistry of the Xining, Xifeng and Jixian sections, Loess Plateau of China: Eolian dust provenance and paleosol evolution during the last 140 ka. Chem. Geol. 178, 71-94.

Kandel, A.W., Felix-Henningsen, P., Conard, N.J., 2003. An overview of the spatial archaeology of the Geelbek Dunes, Western Cape, South Africa. In: Füleky, G. (Eds.), Papers of the 1st Interntional Conference on Archaeology and Soils. Hungary: BAR International Series, pp. 37-44.

Kuman, K., Field, A.S., 2009. The Oldowan industry from Sterkfontein Caves, South Africa. In: Schick, K., Toth, N. (Eds.), The cutting edge: New approaches to the archaeology of human origins. Indiana: Stone Age Institute Press, pp. 151-169.

Leakey, M.D., 1971. Olduvai Gorge. Excavations in Beds I and II, 1960e1963, vol. 3.Cambridge University Press, Cambridge.

Lenoble, A., Bertran, P., 2004. Fabric of Paleolithic levels: methods and implications for site formation processes. J. Archaeol. Sci. 31, 457-469.

Lerman, A., 1978. Lakes Chemistry, Geology, Physics. Berlin: Springer.

Li, H., Li, C.R., Kuman, K., 2016. Site Formation Analysis of Guochachang II Palaeolithic Site in Danjiangkou Reservoir Region. Jianghan Archaeol. 142, 42-50.

Li, T.Y., Mo, D.W., Zhu, G.R., Wang, H.B., Zhang, Y.F., Guo, Y.Y., 2013. Geochemical characteristics of major elements and its paleoenvironmental significance of Holocene loess profile in southern Shanxi, China. Geographical Research 32, 1411-1420.

Li, Z.Y., 2007. A primary study on the stone artifacts of Lingjing site excavated in 2005. Acta. Anthropol. Sin. 26, 138-154.

Li, Z.Y., 2010. 2006 excavation on the Paleolithic Lingjing site in Xuchang. Acta. Archaeol. Sin. 1, 73-100.

Li, Z.Y., 2009. Archaeological discovery and exploration at the Lingjing Xuchang hominid site in Xuchang, Henan. Huaxia Archaeol. 89, 3-7.

Li, Z.Y., Dong, W., 2007. Mammalian fauna from the Lingjing Paleolithic site in Xuchang, Henan Province. Acta. Anthropol. Sin. 26, 345-360.

Li, Z.Y., Shen, C., 2010. Use-wear analysis confirms the use of Paleolithic bone tools by the Lingjing Xuchang early human. Chinese. Sci. Bull. 55, 895-903.

Li, Z.Y., Wu, X.J., Zhou, L.P., Liu, W., Gao, X., Nian, X.M., Trinkaus, E., 2017. Late Pleistocene archaic human crania from Xuchang, China. Science 355(6328), 969-972.

Li, Z.Y., Zhang, S.Q., Zhang, Y., Gao, X., 2011. Mortality curves for horses (Equus Caballus) from the Lingjing site, Henan Province. Acta. Anthropol. Sin. 30, 45-54.

Liu, D.S., 1985. Loess and Environment. Science Press, Beijing.

Liu, D.S., 1997. Quaternary Environment. Science Press, Beijing.

Liu, X.M., Rolph, T., Bloemendal, J., Shaw, J., Liu, T.S., 1995. Quantitative estimates of palaeoprecipitation at Xifeng, in the Loess Plateau of China. Palaeo. Palaeo. Palaeo. 113, 243-248.

Liu, X.X., Vandenberghe, J., An, Z.S., Li, Y., Jin, Z.D., Dong, J.B., Sun, Y.B., 2016. Grain size of Lake Qinghai sediments: Implications for riverine input and

Holocene monsoon variability. Palaeo. Palaeo. Palaeo. 449, 41-51.

Lotter, M.G., Gibbon, R.J., Kuman, K., Leader, G.M., Forssman, T., Granger, D.E., 2016. A geoarchaeological study of the Middle and Upper Pleistocene levels at Canteen Kopje, Northern Cape Province, South Africa. Geoarchaeology 31, 304-323.

Lu, H.Y., An, Z.S., 1998. Paleoclimatic significance of grain size of loess-palaeosol deposit in Chinese loess plateau. Sci. China Ser. D Earth Sci. 41 (6), 626–631.

Maher, B.A., Thompson, R., 1995. Paleorainfall reconstruction from pedogenic magnetic susceptibility variations in the Chinese Loess and paleosols. Quat. Res. 44, 383-391.

McBrearty, S., 1990. Consider the humble termite: termites as agents of post-depositional disturbance at African archaeological sites. J. Archaeol. Sci. 17, 111-143.

McBrearty, S., Bishop, L., Plummer, T., Dewar, R., Conard, N., 1998. Tools underfoot: human trampling as an agent of lithic artifact edge modification. American Antiquity 63, 108-129.

McNabb, J., Kuman, K., 2015. Experimental stone tool replication at the Early Stone Age site of Sterkfontein, Gauteng, South Africa. J. Archaeol. Sci. Reports 4, 44-53.

McPherron, S., 2005. Artifact orientations and site formation processes from total station proveniences. J. Archaeol. Sci. 32, 1003-1014.

Min, L.R., Chi, Z.Q., 2003. Quaternary Geology of the West of Yangyuan Basin in Hebei. Geology Press, Beijing.

Moeyersons, J., 1978. The behaviour of stones and stone implements, buried in consolidating and creeping Kalahari sands. Earth Surface Processes and Landforms 3, 115-128.

Morton, A.G.T., 2004. Archaeological Site Formation: Understanding Lake Margin Contexts. BAR International Series, Oxford.

Nesbitt, H.W., Young, G.M., 1982. Early Proterozoic climates and plate motions inferred from major element chemistry of lutites. Nature 229, 715-717.

Nielsen, A.E., 1991. Trampling the archaeological record: an experimental study. American Antiquity 56, 483-503.

Pei, S.W., Niu, D.W, Guan, Y., Nian, X.M., Kuman, K., Bae, C.J., Gao, X., 2014. The earliest Late Paleolithic in North China: site formation processes at Shuidonggou Locality 7. Quat. Int. 347, 122-132.

Pei, S.W., Niu, D.W., Guan, Y., Nian, X.M., Yi, M.J., Ma, N., Li, X.L., Sahnouni, M., 2015. Middle Pleistocene hominin occupation in the Danjiangkou Reservoir Region, Central China: studies of formation processes and stone technology of Maling 2A site. J. Archaeol. Sci. 53, 391-407.

Petraglia, M.D., Potts, R., 1994. Water flow and the formation of early Pleistocene artifact sites in Olduvai Gorge, Tanzania. J. Anthropol. Archaeol. 13, 228-254.

Potts, R., 1988. Early Hominid Activities at Olduvai. Aldine and Gruyter, New York.

Schick, K.D., 1984. Processes of Palaeolithic Site Formation: An Experimental Study. Ph.D. Dissertation, University of California, Berkeley.

Schick, K.D., 1986. Stone Age Sites in the Making: Experiments in the Formation and Transformation of Archaeological Occurrences. Oxford.

Schick, K.D., 1987, Experimentally derived criteria for assessing hydrologic disturbance of archaeological sites. In: Nash, D.T., Petraglia, M.D. (Eds.), Natural Formation Process and the Archaeological Record. BAR International Series 352, Oxford, pp. 86-107.

Schick, K.D., 1991. On making behavioural inferences from early archaeological sites. In: Clark, J.D. (Eds.), Cultural Beginnings. Dr. Rudolf Habelt GMBH, Bonn, pp. 79-107.

Schick, K.D., 2001. An examination of Kalambo Falls Acheulean Site B5 from a geoarchaeological perspective. In: Clark, J.D. (Eds.), Kalambo Falls Prehistoric Site, III: The Earlier Cultures: Middle and Earlier Stone Age. Cambridge University Press, Cambridge, pp. 463-480.

Schiffer, M.B., 1983. Towards the identification of formation processes. Am. Antiq. 48, 675-706.

Shea, J.J., 1999. Artifact abrasion, fluvial processes, and “living floors” from the

Early Palaeolithic site of Ubeidiya (Jordan Valley, Israel). Geoarchaeology 14, 191-207.

Song, Y.H., Cohen, D.J., Shi, J.M., Wu, X.H., Kvavadze, E., Goldberg, P., Zhang, S.Q., Zhang, Y., Bar-Yosef, O., 2017. Enviromental reconstruction and dating of Shizitan 29, Shanxi Province: An early microblade site in north China. J. Archaeol. Sci. 79, 19-35.

Stahlschmidt, M.C., Miller, C.E., Ligouis, B., Goldberg, P., Berna, F., Urban, B., Conard, N.J., 2015. The depositional environments of Schöningen 13 II-4 and their archaeological implications. J. Hum. Evol. 89, 71-91.

Stein, J.K., 1987. Deposits for Archaeologists. In: Schiffer, M.B. (Eds.), Advances in Archaeological Method and Theory. Academic Press, New York, pp. 337-395.

Toffolo, M.B., Brink, J.S., Huyssteen, C., Berna, F., 2016. A microstratigraphic reevaluation of the Florisbad spring site, Free State Province, South Africa: Formation processes and paleoenvironment. Geoarchaeology 32, 456-478. Xiao, J.L., Fan, J.W., Zhou, L., Zhai, D.Y., Wen, R.L., Qin, X.G., 2013. A model for linking grain-size component to lake level status of a modern clastic lake. J. Asian Earth Sci. 69, 149-158.

Yu, S.H., Zhu, Z.Y., Li, B.Y., Li, S.J., 1998. Preliminary discussion of the climatic record documented in the Fe element of the core samples from Tianshuihai Lake in the last 230 ka, Tibetan Plateau. Marine Geology & Quaternary Geology 18, 63-69.

Yang, L., Sun, Y.J., E, C.Y., Zhao, Y.J., Lu, S.C., 2016. Geochemical element characteristics and paleoenrivonmental significance of aeolian sediments in JXG 1 section. Journal of Salt Lake Research 24, 44-53.

Zhang, S.Q., Gao, X., Zhang, Y., Li, Z.Y., 2011a. Taphonomic analysis of the Lingjing fauna and the first report of a Middle Paleolithic kill-butchery site in North China. Chinese. Sci. Bull. 56, 3213-3219.

Zhang, S.Q., Li, Z.Y., Zhang, Y., Gao, X., 2009. Mortality profiles of the large herbivores from the Lingjing Xuchang Man site, Henan Province and the early emergence of the modern human behaviors in East Asia. Chinese. Sci. Bull. 54,

3857-3863.

Zhang, S.Q., Li, Z.Y., Zhang, Y., Gao, X., 2011b. Cultural modifications on the animal bones from the Lingjing site, Henan Province. Acta. Anthropol. Sin. 30, 313-326.

Zhao, J., Wang, D., Fan, B., Lu, H., Zhang, X., Qu, W., Wen, L., Li, D., 2004. Geochemical characteristics of the loess deposit at Yan'an and its implication to changes of East Asia summer monsoon during the past 130 ka. Geochimica 33, 495-500.